UDK: 623.454.25:62.575
COSATI: 19-01

Computer Simulation and Experimental Testing of the Clock Safety and Arming Device Function

Tatjana Krstić, BSc (Eng)[1)]
Marinko Ugrčić, PhD (Eng)[1)]

Results of continued activities on developing and verifying the method for computer design of the safety and arming device are given. On the basis of the mathematical model of the motion of the safety and arming device given in [1], program code SADFOR for resolving of the differential equations of the motion of the clock mechanism and numerical simulation of its function was developed. Some calculation results with variation of significant parameters of the clock mechanism construction, due to its optimization as well as the arming time performed, are shown. Results of experimental testing of the real model of the mechanism construction that satisfied all functional characteristics as well as the safety performance, thus confirming the quality of the developed method, are also given.

Key words: **fuze, arming device, clock mechanism, safety device, numerical simulation, artillery projectile, construction optimizing.**

Denotations and abbreviations

A_1 to A_{59} – coefficients depending on geometrical and kinematics parameters of all components of the mechanism
e_r – coefficient of restitution
F_{12} – normal contact force between the gear of rotor and smaller gear on pinion no.2
F_{23} – normal contact force between gear no.2 and smaller gear on pinion no.3
I_1 – moment of inertia of the rotor
I_2 – moment of inertia of gears and pinion no.2
I_3 – moment of inertia of the escape wheel and pinion no.3
I_p – moment of inertia of pallet
m_1 – mass of rotor
m_2 – mass of gear and pinion no.2,
m_3 – mass of escape wheel and pinion no.3
m_p – mass of pallet
n – rate of projectile rotation
$\boldsymbol{n}_n, \boldsymbol{n}_t$ – normal and tangent orts
p_n – normal contact force between the escape wheel and pallet
r_{b2} – radius of pinion no.2
r_{b3} – radius of escape wheel pinion
R_{b1} – radius of basic circle of the rotor
R_{b2} – radius of the basic circle of gear no.2
R_1 – distance of the rotor pivot from spin axis
R_4 – distance of pivot of the pallet from the spin axis
r_{cr} – distance from pivot of the rotor to its center of mass
r_{cp} – pallet eccentricity
s_1, s_2, s_4 and s_5 – signum of function (to determine direction of the friction forces)
s – safety zone
T_2 – D'Alambert force on input wheel
T_3 – D'Alambert force on the escape wheel
$\boldsymbol{V}_{TNf} = VP$ – normal components of velocity in the contact points on the pallet after impact
$\boldsymbol{V}_{SNf} = VS$
a_{en} – inclination angle of entrance working surface of the pallet
a_{ex} – inclination angle of exit working surface of the pallet
y'_p – angle between the positive part of x'-axis and vector $\boldsymbol{n}_4$
μ – coefficient of friction on contact surfaces of all pears of gears (tooth-to-tooth contract) and in bearings of its pinions
μ_1 – coefficient of friction on contact surface of the pallet and escape wheel and in bearings of its pinions
ρ_p – radius of the pallet pinion (pallet pivot)
ρ_1 – radius of the rotor pinion (rotor pivot)
$\phi, \dot{\phi}, \ddot{\phi}$ – rotation angle, angular velocity, and angular acceleration of the escape wheel (instantaneous values)
ϕ_{1C} – rotor angle in the initial position
ϕ_T – cumulative angle of escape wheel rotation
$\psi, \dot{\psi}$ – rotation angle and angular velocity of the pallet
ψ_c – eccentricity angle of the pallet
ω – spin rate of projectile, i.e. of the fuze
SAD – safety and arming device

All others denotations and abbreviations unmentioned in the review given above will be explained in the text.

[1)] Military Technical Institute (VTI), Ratka Resanovića 1, 11132 Belgrade

Introduction

THE clock mechanism (Fig.1) is being used frequently in production of the safety and arming devices for all modern types of fuzes for artillery projectiles due to its precision, physical stability, and above all its reliability. The optimum values of the construction parameters of this very responsible part of the artillery projectiles and relatively complex mechanism is not possible to determine without an appropriate calculating method.

The aim of this paper is to present the logical continuity of the activities (given in [1]) for developing and verifying the method for computer design of the safety and arming device which are:

- creating and compiling the software for solving the system of differential equations of the mechanism motion and computer simulation of its function [2-5],
- varying the significant input parameters and defining the optimum safety and arming device design that will accomplish the main functional requirement, i.e. arming time for the required muzzle safety zone, under given conditions,
- experimental testing of the designed model of safety and arming device, and
- comparative analysis of the calculated and experimental results and quality evaluation of the method for computer design of the safety and arming device.

Software for simulation of function of the safety and arming device named SADFOR is intended for full program of artillery fuzes and is developed on the basis of derived mathematical model given in [1]. The feasibility of computer simulation of the mechanism function requires ability to determine the maximum contact forces for each phase of motion, as well as the instantaneous values of kinematics parameters, rotation time, and total number of revolutions before the arming, for all elements of the mechanism.

Description of the safety and arming device

The subsystem of fuze for safety and arming device (SAD) is a special part of artillery fuze consisting of the mechanism that makes it mechanically break the explosive train in the fuze and absolutely safe and secure during the storage, transportation, and handling as well as in the initial phase of projectile launching. The mechanism makes it possible to reinstate the initial explosive train (arming) only when the projectile has crossed safety distance from the muzzle. The requirement for muzzle safety zone must be a minimum 400 calibers.

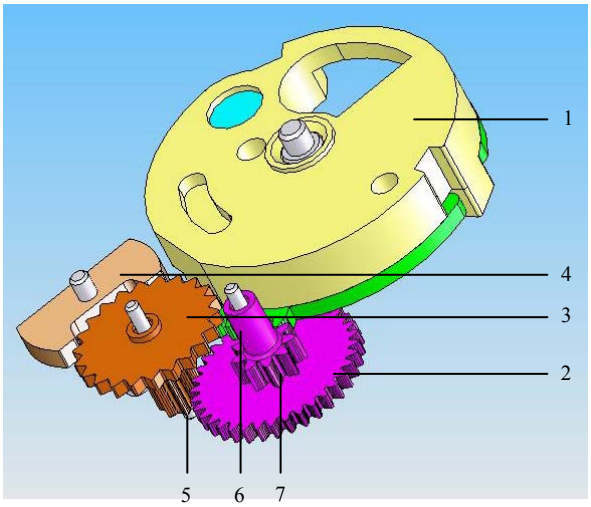

1. Rotor with driving gear no.1; 2. Input wheel (pinion no.2 with gears set no.2, i.e. pallet); 3. Escape wheel (pinion no.3 with gears set no.3); 4. Pallet; 5. Smaller gear in gears set no.3; 6. Cogged segment (driven gear); 7. Smaller gear in gears set no.2

Figure 1. Three-dimensional view and components of the train of coupled gears in the clock mechanism of SAD

The fuze subsystem SAD is a special construction intended for performing safety and arming functions, and considering its universal conception, this device is assigned to complete artillery ammunition of hole caliber from 76mm to 203mm. It consists of the rotor (driven gear), two pears of involutes gears, and a pallet (Fig.1). The mechanism has been estimated to function correctly within a large diapason of loads caused by linear acceleration from 20,000m/s^2 to 250,000m/s^2.

Description of program code SADFOR

Software SADFOR (Fig.2) for solving the system of differential equations of motion and computer simulation of the safety and arming device function was made in FORTRAN computer language, and apart from the main program, includes 9 subroutines.

Subroutines, some of which are not shown explicitly in Fig.2, list as follows:

- ALFA subroutine, intended to calculate the initial values of the kinematics parameters of the mechanism as well as the centrifugal forces in the coupled gears,
- RKGS subroutine, intended to solve the system of differential equations using the Runge-Kutta method of the fourth-order,
- FCT subroutine, intended to calculate the geometrical and kinematical coefficients of the mechanism from A_1 to A_{50} for the phase of coupled motion and functions as a part of the subroutine RKGS,
- FCTS subroutine, intended to calculate the geometrical and kinematical coefficients of mechanism from A_1 to A_{50} for the phase of free motion and functions as a part of the subroutine RKGS,
- IN2 subroutine, intended to calculate the current values of all kinematical parameters included in the systems of differential equations and functions as a part of the subroutines FCT, EXIT, FCTS and EXITS,
- KINEM subroutine, intended to calculate the current values of the rotation angle, angular velocity, and legs of forces at the contact points in the train of gears and functions as a part of the subroutine FCT and EXIT,
- EXIT subroutine, intended to calculate the current values of the kinematical parameters of the escape wheel and pallet as well as the contact forces in the phase of the coupled motion and functions as a part of the subroutine RKGS,
- EXITS subroutine, intended to calculate the current values of the kinematical parameters of the escape wheel and pallet as well as the contact forces in the phase of free motion and functions as a part of the subroutine RKGS,
- IMPACT subroutine, intended to calculate the current values of the kinematical parameters of the escape wheel and pallet after impact.

The main program starts by reading all the relevant geometrical and physico-mechanical data for all components of the mechanism. Than, the main program follows the subroutine ALFA for computation of the gear ratios, initial values of mechanism angles, centrifugal forces, and contact slope in the train of coupled gears. The numerical simulation of the clock mechanism motion begins with the calculation of the para-

meters of the entrance-coupled motion for the given starting angle of the escape wheel ϕ, simultaneously resolving the differential equations for dynamics of motion and impact

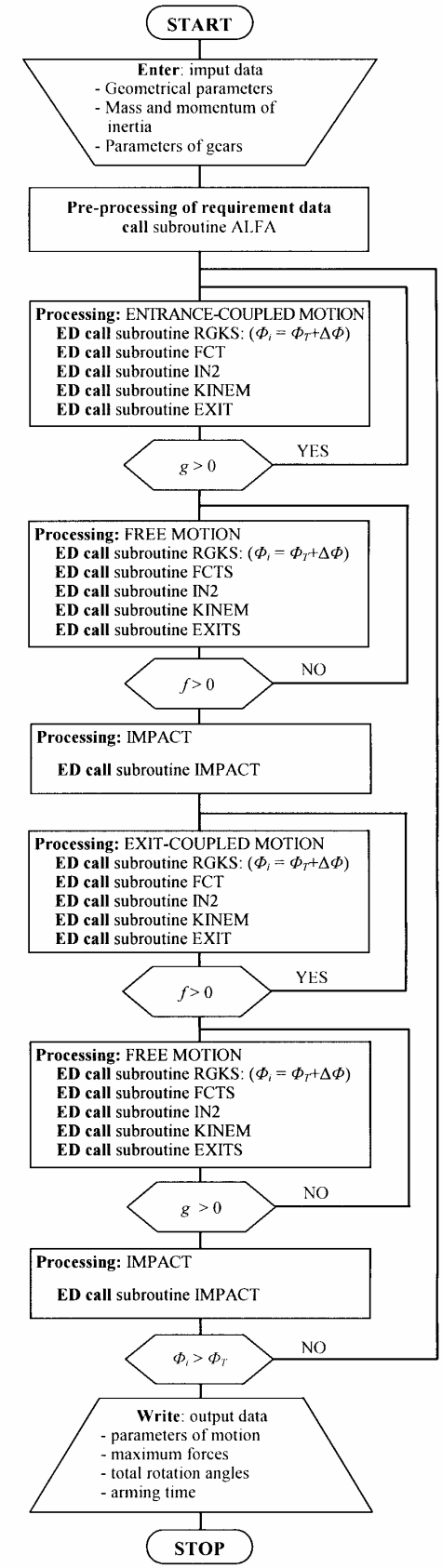

Figure 2. Flow chart of the program SADFOR for solving the defferential equations of motion and numerical simulation of the clock mechanism

mechanics. The initial values of rotation angle for the escape wheel are determined from a condition that considers the contact of the top of the escape wheel and approximate center of the pallet entrance-working surface, at the moment $t = 0$.

It is important to note that this values of the angle (later) corresponds the cumulative rotation angle of the escape wheel ϕ_T.

In the further phase, the program runs as a function of the increment of the escape wheel angle $\Delta\phi$. The basic loops of the program appear with actual phase of the mechanism motion and depend on the connection state in the clock mechanism train which is determined by the instantaneous values of the total rotation angle of the escape wheel ϕ_T. Each phase of the motion: coupled motion, free motion, and impact, has been considered individually.

Coupled motion

Leaving the subroutine ALFA, the program continues to calculate the parameters for the phase of coupled motion. Depending on the type of motion, i.e. whether entrance or exit coupled motion there takes place [1], the program is being solved through differential equations

$$\begin{aligned}&\left[I_3A_{18}+I_{PR}A_{17}U\right]\ddot{\phi}+\left[I_{PR}A_{17}V+A_{17}A_{21}U^2\right]\dot{\phi}^2+2\frac{\omega^2}{|\omega|}A_{17}A_{20}U\dot{\phi}=\\&=A_{15}A_{18}F_{23}-A_{16}A_{18}T_3-A_{17}\omega^2\left[A_{19}-m_pr_{cp}R_4\sin\left(\gamma'_p-\psi-\psi_c\right)\right]\end{aligned}\tag{1}$$

$$\begin{aligned}&\left[I_3AA_{18}+I_{PR}AA_{17}U\right]\ddot{\phi}+\left[I_{PR}AA_{17}V+AA_{17}A_{21}U^2\right]\dot{\phi}^2+\\&+2\frac{\omega^2}{|\omega|}AA_{17}A_{20}U\dot{\phi}=A_{15}AA_{18}F_{23}-A_{16}AA_{18}T_3-\\&-AA_{17}\omega^2\left[A_{19}-m_pr_{cp}R_4\sin\left(\gamma'_p-\psi-\psi_c\right)\right]\end{aligned}\tag{2}$$

The eq.(1) and (2), which describe the entrance-coupled motion or exit-coupled motion for the pallet and escape wheel, were resolved using the numerical Runge-Kutta method of the fourth-order, called the subroutine RKGS. The mentioned subroutine called FCT subroutine apart from its main purpose, transforms the second-order differential equations in terms of two first-order equations, adapted for solving by RKGS subroutine. The calculation of all current parameters is performed on the basis of the system of differential equations using the FCT, IN2 and KINEM subroutines.

In this phase the subroutine KINEM computes current values of the parameters ψ and $\dot{\psi}$, as well as the moment arms A'_1, B'_1, C'_1, and D'_1. The moment arms A'_1, B'_1, C'_1 and D'_1 represent instantaneous values of the shortest distances of the attack point of interactive forces between the coupled components in the gears train from the proper rotation axis, including the rotor, gear 1, and pallet, respectively. The IN2 subroutine calculates different kinematical parameters of the coupled gears and the instantaneous contact of the angle in the gear trains as well as *signum* of the functions s_1, s_2, s_4, and s_5. Apart from the mentioned, in interaction with FCT subroutine (that calculates values of the coefficients from A_{45} to A_{50}) this subroutine calculates values of the coefficients from A_1 to A_{44}. It must be emphasized that the values of the coefficients A_1, A_5, A_9, A_{17}, and A_{18} depend on the instantaneously active phase of the motion, i.e. whether entrance-coupled or exit- coupled motion there takes place. All data, concerning the calculation of the gears parameters, peformed using the above mentioned subroutines, represent the constants or functions of the angle ϕ.

The instantaneous rotation angle of rotor, which appears

in the differential equation of the coupled motion, in the main program, is given by equation

$$\phi_{1C} = \phi_{1C} + N_{31}\phi_T \tag{3}$$

where N_{31} is gear transmission ratio for complete mechanism (from the rotor to the escape wheel).

The rotation angle ϕ, as Runge-Kutta variable, is varying approximately between 1328 and 1468 during entrance-coupled motion and between 2098 and 2168 during exit-coupled motion.

The total rotation angle of the escape wheel ϕ_T represents the sum of the initial values of this angle and increments that are addied continuously during each cycle of Runge-Kutta computations, concordant equation

$$\phi_T \cdot \phi_{TOT} \cdot 1\Delta\phi \tag{4}$$

where ϕ_{TOT} is the total escape wheel rotation angle which is obtained by Runge-Kutta method.

The increment $\Delta\phi$ is calculated as difference between the latest and previous value of this angle, and is stored as a variable under special name *PHIPR*.

In addition, the FCT subroutine calculates the values I_{PR} and I_{1R} according to the equations for coupled entrance motion

$$I_{PR} = I_P + A_{22} \tag{5}$$

where the same sign precedes the $\dot{\psi}$ and $\ddot{\psi}$ and

$$I_{PR} = I_P - A_{22} \tag{6}$$

where the opposite signs precede the $\dot{\psi}$ and $\ddot{\psi}$, according to the equations for coupled exit motion

$$I_{1R} = I_1 + |\mu|\rho_1\left(A_{26} + A_{30}\right) \tag{7}$$

where the same sign precedes the $\dot{\psi}$ and $\ddot{\psi}$ and

$$I_{1R} = I_1 - |\mu|\rho_1\left(A_{26} + A_{30}\right) \tag{8}$$

where the opposite signs precede the $\dot{\psi}$ and $\ddot{\psi}$.

The subroutine EXIT calculates output data for current values of ϕ, $\dot{\phi}$ and $\ddot{\phi}$, as well as for variables *t*, *g*, ψ, $\dot{\psi}$, and ϕ_T. The subroutine calculates the instantaneous values of all contact forces in the phase of the coupled motion by expressions (5) - (8) as well as its maximum values during one cycle of rotor motion by the following eq. [1]

$$\begin{aligned} &F_{23}R_{b2} - \mu s_2 F_{23}a_2 - F_{12}r_{b2} + \mu s_1 F_{12}\left(d_1 - a_1\right) + \\ &+\mu\rho_2\left(F_{x2} + F_{y2}\right) = I_2 N_{32}\ddot{\phi} \end{aligned} \tag{9}$$

$$P_n = \frac{-I_3\ddot{\phi} + F_{23}A_{15} - T_3A_{16}}{A_{17}} \tag{10}$$

$$P_n = \frac{-I_3\ddot{\phi} + F_{23}A_{15} - T_3A_{16}}{AA_{17}} \tag{11}$$

Free motion

Having calculated the parameters for the entrance-coupled entrance motion, the program continues to run on the phase of free motion. The independent differential equations of dynamics for pallet and set, consisting of the rotor coupled with a train of gears, in the phase of free motion take the forms

$$A_{51}\ddot{\psi} + A_{21}\dot{\psi}^2 + A_{52}\dot{\psi} = -A_{53} + A_{54}\sin\left(\gamma_p' - \psi - \psi_c\right) \tag{12}$$

$$A_{55}\ddot{\phi} + A_{56}\dot{\phi}^2 + A_{57}\dot{\phi} = A_{58} - A_{59}\sin\left(\phi_{1c} + N_{31}\phi_T\right) \tag{13}$$

The eq.(12) and (13) are solved by Runge-Kutta method depending on the ϕ and χ, as well as its first time derivatives in this phase of motion, they are translated into differential equations of the first-order. These four unique differential equations of the first-order are solved simultaneously for identical time intervals.

In the FCTS subroutine, differential equations of the first order represent four expressions in the form

$$DX(1) = X(2) : (=\dot{\phi})$$

$$DX(3) = X(4) : (=\dot{\psi})$$

$$\begin{aligned} DX(2) &= \frac{1}{A_{55}}\left[-A_{56}(X(2))^2 + A_{57}X(2) + A_{58}\right] + \\ &+\frac{1}{A_{55}}\left[A_{59}\sin(\phi_{1C} + N_{31}(\phi_T + X(1) - PHIPR))\right] : (=\ddot{\phi}) \end{aligned}$$

$$\begin{aligned} DX(4) &= \frac{1}{A_{51}}\left[-A_{21}(X(4))^2 - A_{52}X(4) - A_{53}\right] + \\ &+\frac{1}{A_{51}}\left[A_{54}\sin(\gamma_p' - \psi - \psi_C)\right] : (=\ddot{\psi}) \end{aligned}$$

Although, at first it may look, they are linked only by the first and third equation, i.e. second and fourth equation, but regarding the fact that the variables ϕ and χ are interlinked indirectly, its solutions as well as the first and second derivatives are carried out for identical time intervals and, in that way, they are compatible.

The FCTS subroutine, in this running phase, computes coefficients from A_{51} to A_{59} and introduces the IN2 subroutine to determine all others coefficients and parameters in the gear trains.

The EXITS subroutine calculates the values of the contact forces during free motion by equations

$$F_{F23} = \frac{I_3\ddot{\phi} + T_3A_{16}}{A_{15}} \tag{14}$$

$$F_{F12} = \frac{F_{F23}A_{44} + T_2A_{43} - I_2N_{32}\ddot{\phi}}{A_{42}} \tag{15}$$

The subroutine IN2, at the same time calculates coefficients from A_{51} to A_{59} and determines the maximum values of the contact forces. The output parameters of the subroutine EXITS are: ϕ_T, *t*, ϕ, $\dot{\phi}$, ψ, and $\dot{\psi}$.

When values of the control parameters *g* and *f* achieve the some value different from zero ($g \neq 0$ or $f \neq 0$), is when the phase of free motion finishes, the EXITS subroutine stops to run and directs further flow of the program to the impact phase.

Impact

After calculating parameters for free motion, the program continues to run on solving the equations that describe

the next phase of mechanism motion, i.e. the impact.

The IMPACT subroutine uses the current values of the angular velocity of the escape wheel and pallet $\dot{\phi}_i$ and $\dot{\psi}_i$ as input parameters of impact and calculates relevant values of the angular velocity after the impact $\dot{\phi}_f$ and $\dot{\psi}_f$ by terms

$$\dot{\phi}_f = \frac{\dot{\phi}_i \left(I_3 D_1' + e_r I_p A_1' \right) + \dot{\psi}_i I_p A_1' \left(1 - e_r \right)}{I_p A_1'^2 + I_3 D_1'^2} \tag{16}$$

and

$$\dot{\psi}_f = \frac{\dot{\phi}_f A_1' + e_r \left(\dot{\psi}_i D_1' - \dot{\phi}_i A_1' \right)}{D_1'} \tag{17}$$

Depending on the values of the coefficient of restitution e_r in eqs. (16) and (17), the IMPACT subroutine can consider this phase as a case of ideal elastic impact (e_r=0) or case of real impact with non-elastic rebound (e_r>0).

Input data

Input data concerning the geometrical, physico-mechanical, and kinematical parameters of the clock mechanism components of the SAD are shown in Tables 1-4.

Table 1. Geometrical parameters of the pallet and escape wheel

No.	Dimension	Denotation	Measure unit	Value
1.	distance between pinions OP and Os	a	mm	5.656
2.	radius of escape wheel	b	mm	4.25
3.	radius of the pallet	c	mm	3.332
4.	angle of entrance working surface	α_{en}	8	42.7131
5.	angle of exit working surface	α_{ex}	8	30.2869
6.	teeth number of the escape wheel coupled with pallet	NT	-	4
7.	coefficient of restitution	e_r	-	0
8.	angle between entrance and exit working surface of the pallet	λ	8	94.574
9.	teeth number of escape wheel	N	-	22

Table 2. Mass and momentum of inertia of clock mechanism components

No.	Dimension	Denotation	Measure unit	Value
1.	mass of rotor	m_1	x10^{-3} kg	2.3249
2.	mass of gear and pinion 2	m_2	x10^{-3} kg	0.1226
3.	mass of escape wheel and pinion 3	m_3	x10^{-3} kg	0.09
4.	mass of the pallet	m_p	x10^{-3} kg	0.2797
5.	momentum of inertia of the rotor	I_1	x10^{-9} kgm^2	0.8487
6.	momentum of inertia of gear and pinion 2	I_2	x10^{-9} kgm^2	1.0597
7.	momentum of inertia of the escape wheel and pinion 3	I_3	x10^{-9} kgm^2	0.5099
8.	momentum of inertia of the pallet	I_p	x10^{-9} kgm^2	2.13088

Table 3. Main geometrical parameters of the clock mechanism

No.	Dimension	Denotation	Measure unit	Value
1.	distance between the axis of rotor and center of mass of the rotor	r_{c1}	mm	1.779
2.	excentricity of the pallet	r_{cp}	mm	0
3.	radius of the pinion of the pallet	ρ_P	mm	0.55
4.	number of revolution till arming	RPM	o/min	3 200
5.	angle of the rotor in initial position	ϕ_{1C}	°	-118.98
6.	angle between x-axis and center of mass of the pallet	ψ_C	°	0
7.	angle of escape wheel at the beginning of coupled motion	$PHID$	°	139
8.	cumulative angle of the escape wheel	PHICUTD	°	1496.3
9.	kinematical coefficient of friction at contact surfaces of metallic gears (pinion and contact tooth-tooth)	μ	-	0.10
10.	coefficient of friction in the phase of impact of the escape wheel and pallet	μ_1	-	0.10

The cumulative rotation angle of the escape wheel PHICUTD is defined as the product of the total rotation angle of the rotor (working angle of rotor) and total transmission ratio of the gears train in the mechanism, as follows

$$PHICUTD = \phi_{1C} PN = 1496.3^{\circ} \tag{18}$$

where

$\phi_{1C} = 46.76^{\circ}$ - working angle of the rotor and

$PN = 32$ - total transmission ratio of gears train.

Table 4. Parameters of gears

No.	Dimension	Denotation	Measure unit	Value
1.	module of gears set no.1 (rotor and pinion 2)	p_{d1}	-	32
2.	module of gears set no.2 (gear 2 and pinion of escape wheel)	p_{d2}	-	25
3.	number of teeth of the rotor (for full circle of gear)	N_{G1}	-	64
4.	number of teeth of gear 2	N_{G2}	-	36
5.	number of teeth of the smaller gear on pinion 2	N_{P2}	-	9
6.	number of teeth of the smaller gear on pinion 3	N_{P3}	-	8
7.	radius of kinematical circle of the rotor	R_{P1}	mm	10.4485
8.	radius of kinematical circle of gear 2	R_{P2}	mm	4.8308
9.	radius of kinematical circle of the smaller gear on pinion 2	r_{p2}	mm	1.4693
10.	radius of kinematical circle of the smaller gear on pinion 3	r_{p3}	mm	1.0735
11.	tangent angle of gears set no.1	υ_1	°	22.96
12.	tangent angle of gears set no.2	υ_2	°	28.915
13.	distance between rotation axis and axis of rotor	R_1	mm	6.350
14.	distance between rotation axis and axis of gear 2	R_2	mm	8.0391
15.	distance between rotation axis and axis of the escape wheel	R_3	mm	7.7980
16.	distance between rotation axis and axis of the pallet	R_4	mm	7.7006
17.	radius of the pinion of the rotor	ρ_1	mm	1.265
18.	radius of the pinion of gear 2	ρ_2	mm	0.4
19.	radius of the pinion of the escape wheel	ρ_3	mm	0.4
20.	radius of the basic circle of the rotor	R_{b1}	mm	9.62
21.	radius of the basic circle of gear 2	R_{b2}	mm	4.2286
22.	radius of the basic circle of smaller gear on pinion 2	r_{b2}	mm	1.35316
23.	radius of the basic circle of the smaller gear on pinion 3	r_{b3}	mm	0.93969
24.	outside radius of rotor	R_{01}	mm	10.53
25.	outside radius of gear 2	R_{02}	mm	4.93
26.	outside radius of the smaller gear on the pinion 2	r_{02}	mm	1.96
27.	outside radius of the smaller gear on the the pinion 3	r_{03}	mm	1.395

Output data

A brief review of the main output data for each phase of the motion is given here.

The coupled motion starts by first contact of the tooth on the escape wheel and entrance of the working surface of the pallet. In this phase of the coupled motion, during time interval T the further kinematical parameters are calculated: ϕ, $\dot{\phi}$, g, ψ, $\dot{\psi}$, ϕ_T, F_{23}, F_{12}, P_n, and $\ddot{\phi}$. During the free motion the values of the current parameters: ϕ, $\dot{\phi}$, ψ, $\dot{\psi}$, ϕ_T, F_{F23}, and F_{F23} are calculated, as well.

The impact of the tooth on the escape wheel and exit-working surface of the pallet follows the phase of free motion. Before the computation of the parameters for this motion phase, the values $VP5V_{TNi}$ and $VS5V_{SNi}$ are calculated. Thay represent normal components of the velocity on the contact point of the pallet and escape wheel before the impact and they are orthogonal onto the working surface of the pallet. This fact, considered along with ϕ, $\dot{\phi}$, ψ, $\dot{\psi}$, and ϕ_T, as well as the normal components of the velocity of the pallet and escape wheel (VP=V_{TNf} and VS=V_{SNf}) on the contact point become the output data of the impact phase after the impact.

Important general data concerning the functioning of the OAM is the number of fuze revolution (i.e. rotation of projectile) until the arming along with maximum values of the contact forces. The number of fuze revolutions before arming under n=3200°/min rotation of the projectile is possibile to calculate on the basis of the time sequence required so that cumulative rotation angle of the escape wheel achieves the value $PHICUTD$=1496.3°. This value is equal to the product of the time sequence and angular velocity of the projectile: 0.05156 s × (3,200/60) rev/s = 25.8 revolutions.

The maximum contact forces during the entire arming cycle, required to computate the mechanical resistance of the design components of the clock mechanism, are calculated for both coupled motion and free motion phase.

Analyses of the working phases of the clock mechanism during one cycle of motion

The clock mechanism, for which the complete numerical simulation with optimization of the design and functional parameters is performed, is realized in configuration of the SAD shown in Fig.3.

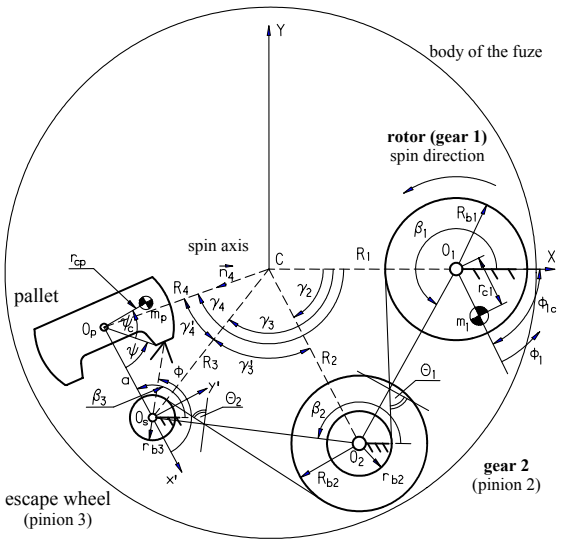

Figure 3. Scheme of safety and arming device with dimensional and main kinematics parameters of mechanism components motion

Further in the text, the description and analysis of the clock mechanism functioning considering the phases of the motion during one full cycle will be briefly exposed. They are given on the basis of the results of numerical simulation where the program SADFOR was used.

Entrance-coupled motion

The coupled entrance motion is characterised by the following:

- In the first step of the entrance-coupled motion, the rotation angle of the escape wheel ϕ takes the value of 139° and in this phase, its values are varying in the interval from approximately 132° to 146°.
- The rotation angle of the pallet ψ is varying in the interval from approximately 41° to 48°.
- The angular velocities of the escape wheel $\dot{\phi}$ and the pallet $\dot{\psi}$ are great as than zero and they have the character of uniformly growing functions.
- The length of the contact entrance working surface g is positive and decreases depending on time.

To start the next phase (free motion) the variable g must be equal zero.

Free motion between entrance and exit motion

The free motion between the phase of the entrance-coupled motion and phase of the exit-coupled motion has the following characteristics:

- The phase starts when parameter g equals zero.
- The phase lasts until the fourth tooth of the escape wheel coupled with pallet touches the exit-working surface of the pallet. The condition for ending this phase of motion is that variable f stays different from zero.
- The rotation angle of the escape wheel grows up to the value of $\phi \approx 210^{\circ}$, that is calculated from the expression

$$\phi = \phi_{fencm} + \frac{360}{22} \cdot 4 \approx 210^{\circ} \tag{19}$$

where ϕ_{fencm} is the final value of the angle ϕ at the end of the entrance-coupled motion.

- The rotation angle of the pallet ψ is variable and is calculated on the basis of the expression

$$\psi = \psi_{fencm} + 2\pi - \lambda \tag{20}$$

where ψ_{fencm} is the final value of the angle ψ at the end of the entrance-coupled motion.

- The angular velocity of the escape wheel $\dot{\phi}$ is positive (great than zero) and increases in time.
- The angular velocity of the pallet $\dot{\psi}$ is positive and decreases in time.

Impact on exit working surface of the pallet

The results of the analysis of computated parameters for the phase of impact on the exit-working surface of pallet shows:

- The calculated values of the normal velocity components of the contact points on the escape wheel (VS) and on the pallet (VP) at the end of the phase of free motion, but immediately before impact, they have the opposite direction (VP>0 and VS<0).

- Immediately after the impact there is *VP*=*VS*, and both velocities take the same direction (*VP*>0 and *VS*>0 or *VP*<0 and *VS*<0).
- The rotation angle of the pallet ψ and rotation angle of the escape wheel ϕ take the initial values that are equal to the values at the end of the phase of free motion.

The numerical simulation of the impact is based on the momentum equations of the classical model of the impact mechanics including the coefficient of restitution e_r to show energy dissipation in the considered material system of the interacting rigid bodies, relevant for the real conditions in which the mechanism works. Considering the negligibly small energy dissipation, it is justified to assume e_r=0. In this case, the angular velocities of the escape wheel and pallet can be calculated by expressions

$$\dot{\phi}_f = \frac{I_N A_1' \dot{\psi}_i + I_{STOT} D_1' \dot{\phi}_i}{I_N \frac{A_1'^2}{D_1'} + I_{STOT} D_1'} \tag{21}$$

$$\dot{\psi}_f = \frac{\dot{\phi}_f A_1'}{D_1'} \tag{22}$$

In this phase $A_1' = b\cos(\phi - \psi - \alpha_{ex})$ is always less than zero, because $\cos(\phi - \psi - \alpha_{ex}) < 0$, but $D_1' = c\cos\alpha_{ex} + g$ is always greater than zero, because $c\cos\alpha_{ex} > g$. Due to the above given facts, opposite signs always precede the angular velocities of the pallet and escape wheel after impact $\dot{\psi}_f$ and $\dot{\phi}_f$.

The sign of $\dot{\phi}_f$ depends on the relation of the expressions $I_N A_1' \dot{\psi}_i$ and $I_{STOT} D_1' \dot{\phi}_i$. If there is $|I_N A_1' \dot{\psi}_i| > |I_{STOT} D_1' \dot{\phi}_i|$ than $\dot{\phi}_f < 0$ and $\dot{\psi}_f > 0$, and *vice versa*.

In the case of the SAD when the pivot of the detonating cap (rotor) and two pears of the involute gears are made of zinc alloy, I_N has the value very close to the I_{STOT}, however smaller to a degree. Due to this relation there is $I_N A_1' \dot{\psi}_i < I_{STOT} D_1' \dot{\phi}_i$, so that the conditions $\dot{\phi}_f < 0$ and $\dot{\psi}_f > 0$ are always satisfied.

In the case of the SAD when the pivot of the detonating cap and two pears of the involute gears are made of plastic mass, I_N is practically four times greater than I_{STOT}, so that the relation of the expressions $I_N A_1' \dot{\psi}_i$ and $I_{STOT} D_1' \dot{\phi}_i$ depends only on the values of the angular velocities of the pallet and escape wheel before the impact.

Considering the possibility that the escape wheel and pallet can move in both directions after impact, concordantly to the relations of the variables *VP* and *VS*:

$$\dot{\phi}_f > 0 \text{ and } \dot{\psi}_f < 0 \Rightarrow VP = VS < 0$$

or

$$\dot{\phi}_f > 0 \text{ and } \dot{\psi}_f > 0 \Rightarrow VP = VS > 0$$

Exit-coupled motion

The exit-coupled motion has the following next characteristics:

- The assumed initial values of the rotation angle of the pallet ψ and rotation angle of the escape wheel ϕ are equal to their final values for the phase of the free inpact.
- The value of the parameter *f* decreases in time until the moment when it achieves zero value, the condition to start free motion phase.
- The angular velocity of the escape wheel $\dot{\phi}$ is positive and increases in time.
- The angular velocity of the pallet $\dot{\psi}$ is negative (pallet moves in a clockwise direction) and decreases in time.

Free motion between exit and entrance motion

The free motion between exit and entrance motion has the following characteristics:

- The phase starts when parameter *f* equals zero.
- The phase lasts until the teeth of the escape wheel touch the entrance-working surface of the pallet. This happens when variable *g* achieves value different from zero. At the same time, it is the condition to exit from this part of program.
- The rotation angle of the escape wheel ϕ varies in the interval from approximately 133° to 140° and is calculated on the basis of the expression

$$\phi = \phi_{fexcm} - \frac{360}{22} \cdot (4+1) \tag{23}$$

where ϕ_{fexcm} is the value of the angle ϕ at the end of the exit- coupled motion.

- The rotation angle of the pallet ψ varies in the interval from approximately (2π-45°) to (2π-42°) and is calculated on the basis of the expression

$$\psi = \psi_{fexcm} - 2\pi + \lambda \tag{24}$$

where ψ_{fexcm} is the value of the angle ψ at the end of the exit-coupled motion.

- The angular velocity of the escape wheel $\dot{\phi}$ is positive and increases depending on time,
- The angular velocity of the pallet $\dot{\psi}$ is negative and increases depending on time.

Impact on the entrance-working surface of the pallet

The impact on the entrance-working surface of pallet has the following characteristics:

- At the end of the free motion phase, the calculated values of the normal components of the contact point velocities on the escape wheel *VS* and pallet *VP*, immediately before the impact, are *VP*<0 and *VS*>0.
- Immediately after the impact they are *VP*=*VS*>0.
- The rotation angle of the pallet ψ and rotation angle of the escape wheel ϕ take the values equal to those at the end of the motion free phase.
- If the value of the rotation angle of the escape wheel is ≈140°, and of the pallet ≈42°, then the angle of the entrance-working surface is α_{en}≈44°. Therefore $\sin\phi > 0$, $\sin\psi > 0$, $\sin(\psi + \alpha_{en}) > 0$, and g>0. A_1' is greater than zero, since the expressions $\cos(\phi - \psi - \alpha_{ex}) > 0$ and $D_1' < 0 \Rightarrow VP = VS < 0 = c\cos\alpha_{ex} + g > 0$

are always greater than zero, so that $\dot{\phi}_i > 0$ and $\dot{\psi}_i < 0$. Considering that $|\dot{\phi}_i|$ is greater than $|\dot{\psi}_i|$, it follows that $I_N A_1' \dot{\psi}_i < I_{STOT} D_1' \dot{\phi}_i$. Finally, this means that the relation $\frac{|\dot{\phi}_i|}{|\dot{\psi}_i|} > \frac{I_N}{I_{STOT}}$ always applies for the variant of the SAD consisting of the components that are made of zinc alloy, because the I_N is approximately equal to I_{STOT}.

- For variant consisting of the pivot of detonating cap, gears, and escape wheel made of plastic mass, I_N is practically four times greater than I_{STOT}, since it might be possible that mechanism made of lighter components (materials of small density) would not function. Therefore, the performed numerical analysis of the mechanism working with plastic components has shown that the computed values of the angular velocities of the escape wheel are significantly greater than the angular velocities of the pallet. Therefore, it can be seen that the above mentioned inequalities are satisfied in this case, as well. At the same time, it results in $\dot{\phi}_f > 0$ and $\dot{\phi}_f > 0$, and because $D_1' > A_1'$, the term $\dot{\phi}_f > \dot{\psi}_f$ is valid. Finally, it can be concluded that the angular velocities of the pallet $\dot{\psi}_f$ and escape wheel $\dot{\phi}_f$ are positive after the impact, where the intensity of the angular velocity of the escape wheel has decreased.

At the same time, this is the last phase of the clock mechanism motion, which represents the end of one full cycle of its functioning. The motion of the mechanism continues by the entrance-coupled motion and by the further periodical repetition of the cycle until the total cumulative rotation angle of the escape wheel would achieve the value *PHICUTD* given by eq.18.

Basic results of numerical simulation of optimized design variants of SAD

The basic computation results of the numerical simulation of the original design of the SAD's optimized variant are presented. There are some components of the clock mechanism (rotor, gear, and escape wheel) made of plastic materials. The materials of high quality: noryl and lexan with 40% of fiberglass have been used in its production. Its physical and chemical characteristics can satisfy very rigorous requirements concerning the resistance to the climate and mechanical influences that affect the mechanism during handling, transportation, and storage as well as the intensive loading during the conditions of use of the mechanism.

The analysis also includes the results of numerical computations of the functioning of the clock mechanism whose components have been made of zinc alloy.

The performed analysis includes three variants of the mechanism:

- **Variant 1**: all components in the train (rotor, gear, and escape wheel) were made of zinc alloy,
- **Variant 2**: rotor was made of zinc alloy, but the gear and escape wheel of lexan, and
- **Variant 3**: rotor was made of noryl, but the gear and escape wheel of lexan.

For each of the three variants some significant input design parameters of the mechanism, which mostly affect the required output parameters of the mechanism motion, have been varied, and they are:

- the radius of the escape wheel *b*,
- the angle between the entrance-working surface and exit-working surface of the pallet λ, (the changes of the angle λ causes variations of the angle of the entrance-working surface α_{en} and angle of the exit-working surface α_{ex} as well as the pallet radius *c*), and
- the dimension L' shown in Fig.4.

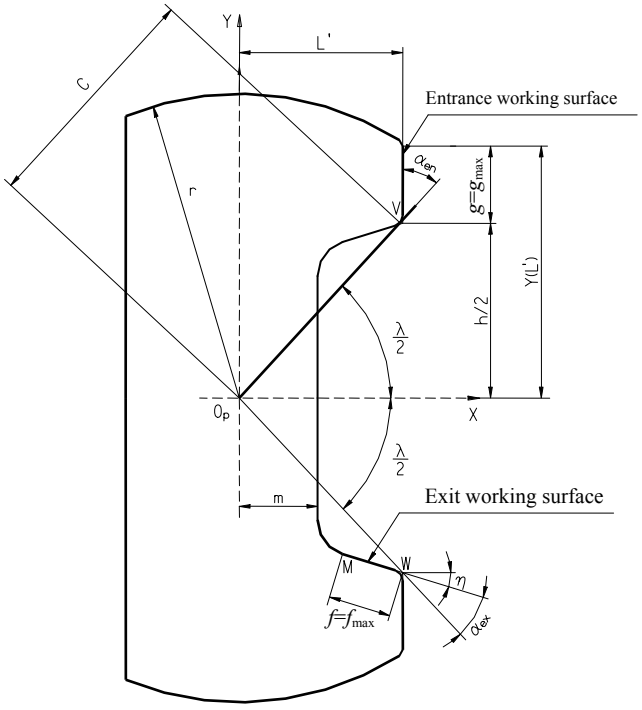

Figure 4. Two-dimensional view and geometrical data of the pallet

The input data and computation results are shown in Tables 5-7.

Table 5. Main geometrical data of the pallet

Function testing under extreme values of acceleration							
No.	Denotation of the input parameter						
	b (mm)	*L'* (mm)	λ (°)	α_{en} (°)	α_{ex} (°)	*c* (mm)	e_r (-)
1	2	3	4	5	6	7	8
1.	4.250	2.30	92.93	43.535	29.465	3.28	0
2		2.30	93.40	43.400	29.700	3.30	0
3		2.30	94.57	42.715	30.285	3.33	0
4		2.25	95.49	42.250	30.430	3.25	0
5		2.30	94.57	42.715	30.285	3.33	0.3
6		2.25	95.49	42.250	30.430	3.25	0.3
7	4.175	2.30	92.93	43.535	29.465	3.28	0
8		2.30	93.40	43.400	29.700	3.30	0
9		2.30	94.57	42.715	30.285	3.33	0
10		2.25	95.49	42.250	30.430	3.25	0
11		2.30	94.57	42.715	30.285	3.33	0.3
12		2.25	95.49	42.250	30.430	3.25	0.3

Table 6. Function testing under minimum acceleration

Initial conditions: n=3200 rev/min and v_0=207 m/s										
		VARIANT 1			VARIANT 2			VARIANT 3		
		Denotation of the input parameter								
No.	b (mm)	t (ms)	n (rev per min)	s (m)	t (ms)	n (rev per min)	s (m)	t (ms)	n (rev per min)	s (m)
1	2	3	4	5	6	7	8	9	10	11
1.	4.250	0.6178	32.95	127.9	0.5877	31.35	121.6	0.8091	43.15	218
2.		0.5979	31.89	123.7	0.5723	30.52	118.5	0.7829	41.75	162
3.		0.5498	29.32	114.0	0.5281	28.17	109.3	0.7105	37.89	147
4.		0.4869	25.97	101.0	0.4357	23.24	90.00	0.5667	30.23	117
5.		0.4168	22.32	86.30	0.3527	18.81	73.00	0.4593	24.50	95.0
6.		0.3804	20.29	78.70	0.3107	16.57	64.00	0.4107	21.90	85.0
7.	4.175	0.4858	25.91	100.5	0.4398	23.46	91.00	0.5719	30.50	118.6
8.		0.4714	25.14	97.58	0.4214	22.47	87.2	0.5430	28.96	114.0
9.		0.4368	23.29	90.42	0.3543	18.90	73.3	0.4283	22.80	88.6
10.		0.3717	19.83	77.00	-	-	-	-	-	-
11.		0.3539	18.88	73.00	0.2630	14.03	54.40	0.3300	17.60	68.0
12.		0.3204	17.09	66.30	0.2113	11.27	43.70	0.2644	14.10	55.0

Table 7. Function testing under maximum acceleration

Initial conditions: n=18000 rev/min and v_0=900 m/s										
		VARIANT 1			VARIANT 2			VARIANT 3		
		Denotation of the input parameter								
No.	b (mm)	t (ms)	n (rev per min)	s (m)	t (ms)	n (rev per min)	s (m)	t (ms)	n (rev per min)	s (m)
1	2	3	4	5	6	7	8	9	10	11
1.	4.250	0.1089	32.69	98.1	0.1044	31.33	94	0..1436	43.08	129
2.		0.1052	31.57	94.7	0.1017	30.51	91.5	0.1393	41.78	125
3.		0.0969	29.08	88.2	0.0939	28.19	84.5	0.1266	37.99	114
4.		0.0857	25.71	77.1	0.0776	23.29	69.9	0.1011	30.33	91.0
5.		0.0736	22.1	66.0	0.0627	18.8	56.5	0.0819	24.58	74.0
6.		0.0672	20.17	60.5	0.0554	16.61	49.8	0.0735	22.04	66.0
7.	4.175	0.0856	25.69	77.1	0.0784	23.51	70.5	0.1021	30.64	92.0
8.		0.0831	24.93	74.8	0.0752	22.55	67.9	0.0968	29.04	87.0
9.		0.0772	23.15	69.5	0.0634	19.01	57.0	0.0766	22.99	69.0
10.		0.0657	18.72	59.1	-	-	-	-	-	-
11.		0.0625	18.7	56.3	0.0469	14.07	42.2	0.0589	17.67	53.0
12.		0.0567	17.01	51.0	0.0378	11.35	34.1	0.0479	14.38	44.0

The influences of the design parameters b and λ on the muzzle safety distance, i.e. the arming zone, under extreme conditions during the initial phase of the projectile flying for all considered variants of the clock mechanism are illustrated graphically (Figures 5 and 6).

On the basis of the diagrams, shown in Figures 5 and 6, realized by numerical simulation of the influence of the significant design parameters of clock mechanism, it is evident that:

- relatively small variations of the geometrical parameters of the pallet (parameter λ in Fig.4) and escape wheel (parameter b), under constant values of other design parameters, show that the muzzle safety distance, as controlled output parameter, has change significantly, so that they can be classified in the category of the most significant factors for the mechanism functioning,
- with increasing of the parameter λ the muzzle safety distance monotonously decreases independently from the conditions of numerical experiment (curves 1- 6), and if acceleration is smaller than the fall-gradient of this, the distance is greater,
- with decreasing of the parameter b the muzzle safety distance stays shorter for all variants of the mechanism not depending on the working conditions (curves 4 - 6 are placed under the relevant curves 1 - 3),
- the variation of the kind of materials of which the mechanism components were made, would not cause changes in the character of the muzzle safety zone in function of the parameters λ and b. Therefore, for the variants of the mechanism made of plastic mass the arming time extends importantly, so that the muzzle safety distance evidently increases (curves 1 and 4 for variant 3), especially with increasing of the parameter b under conditions of the minimum acceleration, and finally
- the increasing of the axial acceleration during launching leads to faster functioning of the mechanism, that causes decreasing of the muzzle safety zone.

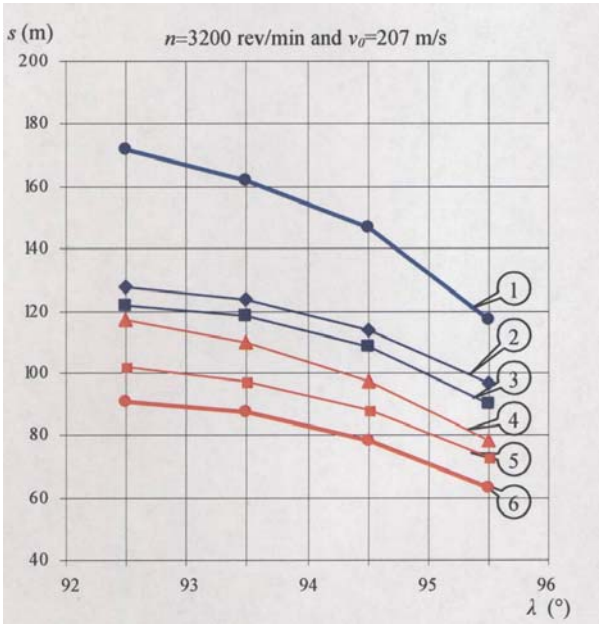

1. b = 4.250 mm, VAR.3
2. b = 4.250 mm, VAR.1
3. b = 4.250 mm, VAR.2
4. b = 4.175 mm, VAR. 3
5. b = 4.175 mm, VAR. 1
6. b = 4.175 mm, VAR. 2

Figure 5. Influence of the clock mechanism design parameters b and λ on muzzle safety zone s under minimum acceleration

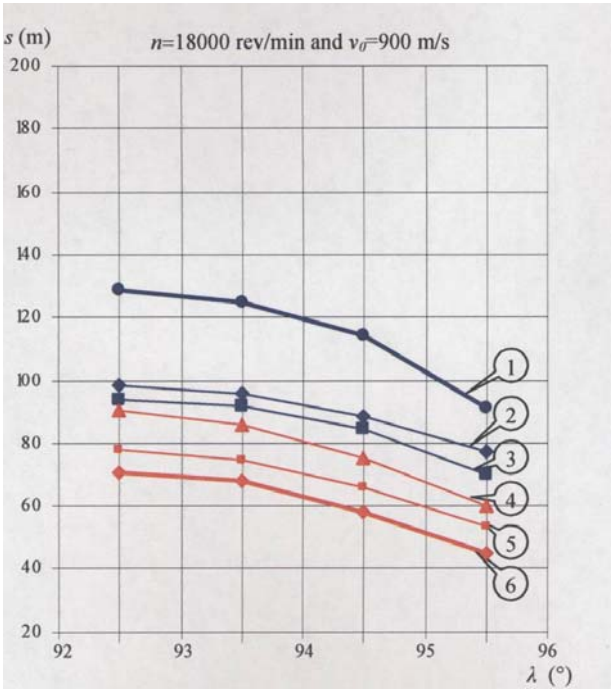

1. b = 4.250 mm, VAR.3
2. b = 4.250 mm, VAR.1
3. b = 4.250 mm, VAR.2
4. b = 4.175 mm, VAR. 3
5. b = 4.175 mm, VAR. 1
6. b = 4.175 mm, VAR. 2

Figure 6. Influence of the clock mechanism design parameters b and λ on muzzle safety zone s under maximum acceleration

Based on the above mentioned statements and the performed analysis of the main results of the numerical simulation of the design for the SAD's optimized variants, it can be concluded that all variants of the mechanism supply a minimum 44 m of the muzzle safety zone.

The numerical simulation of the mechanism function including coefficient of restitution with the value e_r=0.3, was carried out as well. The analysis has shown that in this case the decreasing of the muzzle safety zone from 10 up to 30m would cause somewhat irregular functioning of the mechanism. However, considering the accepted value of the coefficient of restitution that is greater than the real value for the relevant types of the designs, it can be concluded that all the realized models of the mechanism would satisfy the safety requirements.

Basic results of the experimental testing of the design functioning for SAD's optimized variant

The basic experimental testing of SAD's functioning has included testing of safety and arming under extreme loadings. Considering the principle of its universal use in all artillery systems, accepted for SAD's conception, it must satisfy the functional requirements, i.e. regular functioning under the loading caused by the forces that produce the linear accelerations ranging from 20,000m/s^2 to 250,000m/s^2. For this reason a firing test was performed to verify the mechanism's functioning by:

- firing from 76mm and 105mm artillery systems, for the functional verification under conditions of minimum acceleration, and
- firing from 100 mm artillery system, for the functional verification under conditions of maximum acceleration.

For experimental reasons, the SAD was integrated into several types of artillery fuzes, among them the modern type of electronic time fuze (Fig.7) was provided.

Before the firing test, the experimental models of the SAD were verified in laboratory conditions. The reliability of its arming function under extremely small values of rotation n=1600 °/min (projectile velocity was v_0=0) was proven.

The functioning of the SAD, variant 2 (shown in Fig.8), was also tested experimentally under dynamic conditions.

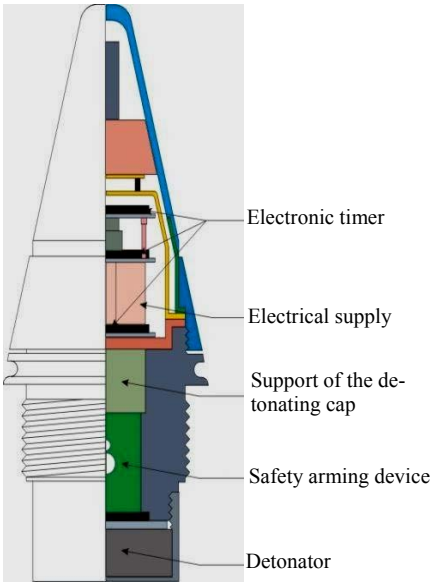

Figure 7. Axial cross-section of modern time fuze with implemented safety arming mechanism

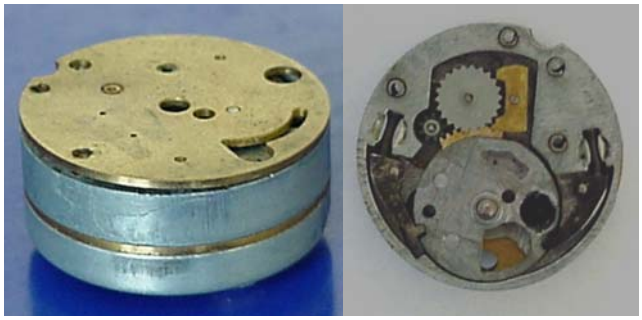

Figure 8. View of the realized design of safety arming device (left) and coupled gears train of the clock mechanism (right)

For this variant, the previous numerical simulation under launching conditions where the mechanism has to work regularly and satisfy the required value of the muzzle safety distance was carried out. The results of the analysis are shown in Table 8.

Table 8. Functional testing under minimum aceleration

Condition of testing							1053400 cal=42 m min.acceleration n=5121rev/min v_0=201 m/s			763400 cal=30.4 m min.aceleration n=7000rev/min v_0=222 m/s		
b (mm)	L' (mm	λ (°)	α_{en} (°)	α_{ex} (°)	c (mm)	e_r (-)	t (s)	N_p^* (rev.)	s (m)	t (s)	N_p (rev.)	s (m)
4.25	2.3	92.93	43.53	29.46	3.28	0	0.3764	32.12	75.6	0.2749	32.07	61
	2.3	93.4	43.4	29.7	3.3	0	0.3639	31.06	73.1	0.2685	31.33	59.6
	2.3	**94.57**	**42.71**	**30.28**	**3.33**	**0**	**0.3349**	**28.58**	**67.3**	**0.2446**	**28.54**	**54.3**
	2.25	95.49	42.25	30.43	3.25	0	0.2757	23.53	55.4	0.2014	23.49	44.7
	2.3	**94.57**	**42.71**	**30.28**	**3.33**	**0.3**	**0.2214**	**18.90**	**44.5**	**0.1619**	**18.89**	**36**
	2.25	95.49	42.25	30.43	3.25	0.3	0.1958	16.71	39.4	0.1433	16.72	31.8
4.205	2.3	92.93	43.53	29.46	3.28	0	0.3182	27.16	63.9	0.2320	27.07	51.5
	2.3	93.4	43.4	29.7	3.3	0	0.3084	26.33	62	0.2254	26.30	50
	2.3	**94.57**	**42.71**	**30.28**	**3.33**	**0**	**0.2729**	**23.30**	**54.8**	**0.1994**	**23.26**	**44.3**
	2.25	95.49	42.25	30.43	3.25	0	0.2069	17.66	41.6	0.1503	17.54	33.4
	2.3	**94.57**	**42.71**	**30.28**	**3.33**	**0.3**	**0.1852**	**15.81**	**37.2**	**0.1354**	**15.79**	**30**
	2.25	95.49	42.25	30.43	3.25	0.3	0.1565	13.36	31.4	0.1141	13.31	25.3

N_p – number of projectile revolutions at the end of arming

The data in bold (Table 8) represent the values of the design parameters of the realized and tested model of the SAD for a supposed ideal elastic impact (e_r=0) and for supposed real case of the impact with an inelastic rebound (e_r=0.3).

The safety testing in front of the gun barrel has been peformed with two groups consisting of five specimens by firing from 76mm artillery system with minimum power charge on the vertical target made of fir boards 25mm thick. At the distance of 30.5m (≈400 calibers), that in this case represents the required muzzle safety zone as well as at the additional distance of 33.5m (≈440 calibers as the safety reserve), no fuzes were activated in collision with the target. It means that the models of the clock mechanism have supplied the required safety function. The arming function was confirmed later by activation of the fuzes on the horizontal target, or more precisely in the contact of the projectile with the ground at the assigned range.

The results of numerical simulation and experimental testing of the muzzle safety zone under conditions of minimum axial acceleration are presented graphically in Fig.9.

Comparative analysis of the results of numerical simulation and experimental testing of the clock mechanism functioning, given in Table 8 and illustrated in diagram (Fig.9), shows:

- Results of the experiment performed under the worst testing conditions i.e. under minimum acceleration, which are in correlation with rotation and muzzle velocity n = 7000rev/min and v_0 = 222m/s, respectively, confirm that the safety zone for artillery system of the smallest, 76mm caliber is more than required 30.5m, i.e. 400 calibers.
- The experimental results are rallied in the area upper value s = 30.5 m (regular requirment for muzzle safety zone S), as well as upper s = 33.5 m (reserve for required muzzle safety zone S) (Fig.9). They are distributed between the calculated values of the muzzle safety zone s = 36m for non-elastic impact and s = 54.3m for ideal elastic impact (Table 8, data in bold for b = 4.250mm), that proves a very good concordance of the theoretical and experimental results.

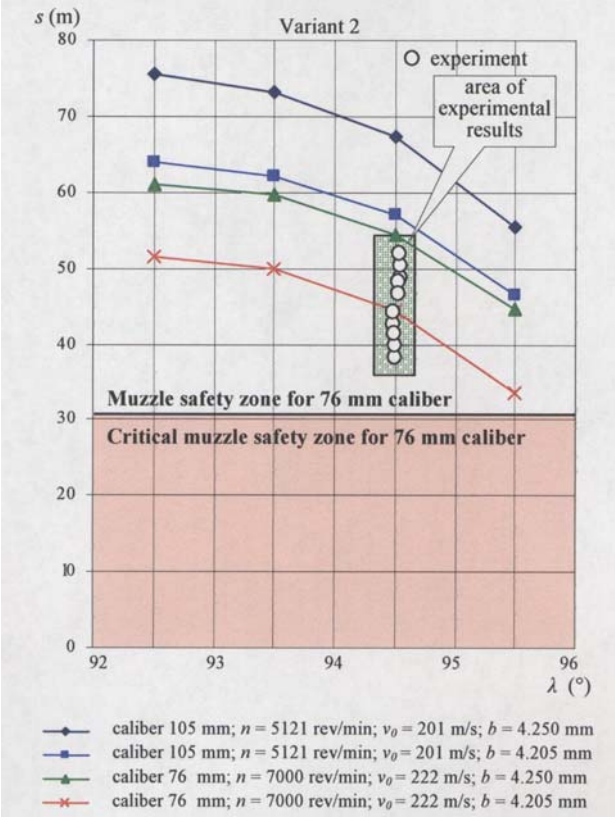

Figure 9. Influence of the clock mechanism design parameters b and λ on the muzzle safety zone s under minimum acceleration

Based on the given statements it can be concluded that the realized model of the clock mechanism, during testing of the muzzle safety zone under conditions of minimum acceleration and in the worst case of its use in real artillery systems, has met functional requirements for the safety in front of the gun barrel. At the same time, these facts confirm the quality of the program code for numerical simulation of the clock mechanism in the SAD.

Conclusion

Based on the results of the theoretical and experimental research, as well as the performed analysis given in this paper which represents the continuation of the activities on the development and verification of the method for numerical simulation and design of the safety arming devices, it can be concluded that:

- The creation and compilation of the software for solving the systems of differential equations of the mechanism motion and for numerical simulation of its functioning was carried out successfully. The software for numerical simulation of the safety-arming mechanism functioning labeled as SADFOR, which covers the complete program of the artillery fuzes, was developed and verified.
- The optimum designs for safety arming devices, based on different constructional materials, were defined using variations of significant input parameters.
- Experimental testing of the real designs of the optimized safety arming devices has shown that the mechanism meets the main assigned requirement, which is arming time necessary to ensure safety in front of the gun barrel.
- The performed comparative analysis of the calculated and experimental results has confirmed the quality of the method for numerical simulation and computer design of the safety arming devices.

The presented reliable method for determining the safety arming device parameters, apart from its contribution to decreasing its development period, also decreases significantly the material expenses of development, because the method makes it possible to avoid the functional control of the mechanism by firing after each correction.

References

[1] KRSTIĆ T., UGRČIĆ M., *Mathematical modeling of motion of the clock safety and arming device*, Scientific-Technical Review, 2005, Vol.LV, No.1.

[2] LOWEN G.G, TEPPER F.R. *Dynamics of the Pin Pallet Escapement*, Technical Report, ARRADCOM, Dover, June, 1982.

[3] LOWE G.G, TEPPER F.R. *Fuze Gear Train Analysis*, Technical Report, ARRADCOM, Dover, December, 1979.

[4] LOWEN G.G, TEPPER F.R. *Computer Simulation of Artillery S&A Mechanism (Involute Gear Train and Pin Pallet Runaway Escapement*), Technical Report, ARRADCOM, Dover, July, 1982.

[5] LOWEN G.G, TEPPER F.R. Computer Simulation of Artillery S&A Mechanism (Involute Gear Train and Straight-side Verge Runaway Escapement), Technical Report, ARRADCOM, Dover, November, 1982.

Received: 10.01.2005.

Numerička simulacija i eksperimentalna provera funkcije satnih osiguravajuće-armirajućih mehanizama

U radu su izloženi rezultati nastavka aktivnosti na razvoju i verifikaciji metode za numeričko projektovanje osiguravajuće-armirajućih mehanizama. Na osnovu matematičkog modela kretanja osiguravajuće-armirajućeg mehanizma prikazanog u [1], urađen je softver OAMFOR za rešavanje diferencijalnih jednačina kretanja satnog mehanizma i numeričku simulaciju njegove funkcije. Prikazani su i određeni rezultati proračuna u kojima su varirani uticajni parametri konstrukcije mehanizma, na osnovu kojih je izvršena njegova optimizacija i ostvareno zahtevano vreme ar-

miranja. Dati su i rezultati eksperimentalnog ispitivanja realizovanog konstrukcionog rešenja koje je zadovoljilo sve funkcionalne karakteristike i zahtev za sigurnost, čime je potvrđena valjanost razvijene metode.

Ključne reči: **upaljač, armiranje upaljača, satni mehanizam, sigurnosni mehanizam, numerička simulacija, optimizacija konstrukcije, artiljerijski projektil.**

Simulation sur ordinateur de la fonction du mécanisme de sûreté et d'armement

Les résultats de la continuité des activités sur le développement et la vérification d'une méthode de modélisation sur ordinateur de la construction du mécanisme de sûreté et d'armement ont été présentés. A la base de modèle mathématique du mouvement de mécanisme de sûreté et de l'armement présenté à [1], le programme numérique OAMFOR pour résoudre des équations différentielles de mouvement du mécanisme d'horloge aussi bien que la simulation numérique de sa fonction ont été effectué. Certains résultats des calculs dans lesquels ont été variés les paramètres signifiants de la construction du mécanisme ont été aussi présentés, afin de faire son optimisation et d'obtenir le délai d'armement demandé. Aussi, les résultats d'évaluation expérimentale de la construction réalisée laquelle a satisfait toutes les caractéristiques fonctionnelles ainsi que l'exigence de sûreté, ont été présentés et de cette façon la validité de méthode développée a été approuvée.

Mots-clés: **fuse de l'artillerie, armament, mécanisme d'une horloge, mécanisme de sûreté, modélisation sur ordinateur, optimisation de la construction, projectile de l'artillerie.**

Численное моделирование и экспериментальная проверка функции часовых предохранительно-подготавливающих механизмов

В этой работе показаны результаты продолжения деятельности на развитии и удостоверении подлинности метода для численного проектирования предохранительно-подготавливающих механизмов. На основании математической модели движения предохранительно-подготавливающего механизма показаного в (1), сделано программное обеспечение ОАМФОР ради решения дифференциальных уравнений движения часового механизма и ради численного моделирования его функции. Здесь показаны и определенные результаты расчетов, в которых даны разновидные влияющие параметры конструкции механизма, на основании которых проведена его оптимизация и вышолнено потребованное время подготавливания. В работе тоже приведены и результаты экспериментального исследования реализованного конструкционного решения, которое удовлетворило всем функциональным характеристикам и требованиям надежности, что потвердило достойность развивающего метода.

Ключевые слова: **взрыватель, подготовка взрывателя, часовой механизм, предохранительный механизм, численное моделирование, оптимизация конструкции, артиллерийский снаряд.**